NAVAL POSTGRADUATE SCHOOL
Monterey, California

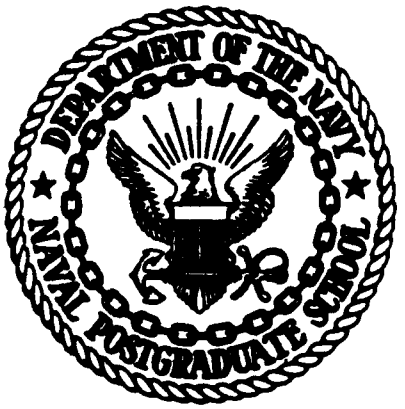

THESIS

A COMPARISON OF TWO EXTENDED KALMAN FILTER ALGORITHMS FOR AIR-TO-AIR PASSIVE RANGING

by

Ward Hubert Ewing

September 1983

Thesis Advisor: J.N. Eagle

Approved for public release; distribution unlimited.

UNCLASSIFIED

SECURITY CLASSIFICATION OF THIS PAGE (When Data Entered)

REPORT DOCUMENTATION PAGE	READ INSTRUCTIONS BEFORE COMPLETING FORM
1. REPORT NUMBER	2. GOVT ACCESSION NO. AD-A136 935	3. RECIPIENT'S CATALOG NUMBER
4. TITLE (and Subtitle) A Comparison of Two Extended Kalman Filter Algorithms for Air-to-Air Passive Ranging	5. TYPE OF REPORT & PERIOD COVERED Master's Thesis; September 1983
	6. PERFORMING ORG. REPORT NUMBER
7. AUTHOR(s) Ward Hubert Ewing	8. CONTRACT OR GRANT NUMBER(s)
9. PERFORMING ORGANIZATION NAME AND ADDRESS Naval Postgraduate School Monterey, California 93943	10. PROGRAM ELEMENT, PROJECT, TASK AREA & WORK UNIT NUMBERS
11. CONTROLLING OFFICE NAME AND ADDRESS Naval Postgraduate School Monterey, California 93943	12. REPORT DATE September 1983
	13. NUMBER OF PAGES 68
14. MONITORING AGENCY NAME & ADDRESS(if different from Controlling Office)	15. SECURITY CLASS. (of this report) Unclassified
	15a. DECLASSIFICATION/DOWNGRADING SCHEDULE

16. DISTRIBUTION STATEMENT (of this Report)

Approved for public release; distribution unlimited.

17. DISTRIBUTION STATEMENT (of the abstract entered in Block 20, if different from Report)

18. SUPPLEMENTARY NOTES

DTIC COPY INSPECTED

19. KEY WORDS (Continue on reverse side if necessary and identify by block number)

Passive Ranging
Bearings-only Ranging
Target Motion Analysis
Kalman Filter
Extended Kalman Filter

Accession For	
NTIS GRA&I	☑
DTIC TAB	☐
Unannounced	☐
Justification	
By	
Distribution/	
Availability Codes	
Dist	Avail and/or Special
A-1	

20. ABSTRACT (Continue on reverse side if necessary and identify by block number)

Two Extended Kalman Filter algorithms for air-to-air passive ranging are proposed, and examined by computer simulation. One algorithm uses only bearing observations while the other uses both bearing and elevation angles. Both are tested using a flat-Earth model and also using a spherical-Earth model where the benefit of a simple correction for the curvature-of-the-Earth effect on elevation angle is examined. The effects of varied

DD FORM 1 JAN 73 1473 EDITION OF 1 NOV 65 IS OBSOLETE
S/N 0102-LF-014-6601

UNCLASSIFIED
SECURITY CLASSIFICATION OF THIS PAGE (When Data Entered)

#20 - ABSTRACT - (CONTINUED)

angle measurement precision and of varied range estimate accuracy are investigated. Both filters are found to perform acceptably under most conditions, with the bearing-elevation algorithm generally providing superior results.

Approved for public release; distribution unlimited.

A Comparison of Two Extended Kalman Filter Algorithms for Air-to-Air Passive Ranging

by

Ward Hubert Ewing
Commander, United States Navy
B.S., North Dakota State University, 1966
M.S., University of Southern California, 1978

Submitted in partial fulfillment of the requirements for the degree of

MASTER OF SCIENCE IN OPERATIONS RESEARCH

from the

NAVAL POSTGRADUATE SCHOOL

September 1983

Author: Ward H. Ewing

Approved by: _____ Thesis Advisor

_____ Second Reader

_____ Chairman, Department of Operations Research

_____ Dean of Information and Policy Sciences

ABSTRACT

Two Extended Kalman Filter algorithms for air-to-air passive ranging are proposed, and examined by computer simulation. One algorithm uses only bearing observations while the other uses both bearing and elevation angles. Both are tested using a flat-Earth model and also using a spherical-Earth model where the benefit of a simple correction for the curvature-of-the-Earth effect on elevation angle is examined. The effects of varied angle measurement precision and of varied range estimate accuracy are investigated. Both filters are found to perform acceptably under most conditions, with the bearing-elevation algorithm generally providing superior results.

TABLE OF CONTENTS

LIST OF TABLES

LIST OF FIGURES

ACKNOWLEDGEMENT

It is a pleasure to acknowledge the inspiration and assistance provided by Dr. James Eagle (Cdr. USNR), Assistant Professor of Operations Research and Systems Analysis. His perseverance and unselfish devotion of time were essential factors in the completion of this study. Additionally, his past experience as a submariner complemented nicely the author's experience in fighter aviation in dealing with a subject area which has application to both communities.

I. INTRODUCTION

The problem of Fleet Air Defense and air defense in general is one covering increasingly large geographical areas due to the greater speeds, ranges, and missile launch envelopes of potentially hostile airborne attack platforms. Concurrent with the expansion of the physical size of the problem has been an increase in its complexity particularly in the area of Electronic Warfare (EW).

A common effect of EW is the denial of range and range rate information by electronic jamming of the observer's radar system. Since target range and range rate must generally be known or at least estimated for a fighter to successfully employ its missile system, the fighter must have some alternate means of obtaining that information.

An approach to this problem is called Passive Ranging (PR) or passive Target Motion Analysis (TMA). This might involve one or more observers using a "receive-only" radar mode or perhaps a highly directional infrared (IR) sensor. It could entail such things as: (a) triangulation of bearing observations from more than one observer, (b) use of one or more known target parameters (with continued bearing observations) to compute the other parameters, (c) use of direct bearing and elevation angle observations in combination with observations of radio frequency (RF) energy reflected

from the water or Earth's surface, and/or (d) a series of observer maneuvers used in conjunction with angular observations.

Determination of a target's position and motion by means of calculations performed on observations of only bearing (and possibly elevation) angles is confounded by the reality that the angle measurements are noisy. That is, while a series of measurements may be centered on the true values, individual measurements will differ from the true values by varying amounts and in a random way. This type of PR problem may be thought of, then, as having two major facets: first, from the series of measurements the observer must make "best guesses" as to the true angle values; and second, using these estimates, he must solve a dynamic geometry problem to ascertain target position and motion.

A "good" system for passive ranging will determine target parameters using only its own observations, but it might reasonably be expected to also make use of any a priori targeting information to improve its speed and/or accuracy of solution. A method for doing this is by means of a Kalman Filter (KF) algorithm in which the prior information is utilized along with an estimate of how accurate that information is. The KF (or, more precisely, the Extended Kalman Filter (EKF)) is successfully employed presently in the submarine and surface ship anti-submarine warfare communities. In this environment observations are normally acoustic bearing measurements, although the use of

depression/elevation angle with "bottom-bounce" reflections has been utilized or proposed.

Representative of current thinking on passive ranging as an air-to-air problem are techniques proposed by Ohlmeyer [Ref. 1], and Stiffler [Ref. 2], which also rely on the use of EKF's. Ohlmeyer's technique uses only bearing angle information, whereas Stiffler presents six different algorithms using bearing-only or a combination of bearing and elevation angle observations.

This paper proposes and investigates methods of passive target motion analysis by means of two EKF's, where both bearing-only and bearing-elevation solutions are computed simultaneously for comparison purposes.

II. THE KALMAN FILTER AND EXTENDED KALMAN FILTER

A. THE KALMAN FILTER

The following discussion briefly describes Kalman Filtering in general, the need in our case for the Extended Kalman Filter, and an application of the EKF to the air-to-air passive ranging problem. The reader interested in a more in-depth development of the KF and EKF is referred to References 3, 4, and 5.

The purpose of a KF is to keep track of the state of a system by means of a sequence of noisy measurements. This is done by recursively updating an estimate of the state by computationally processing the succession of noisy observations in such a way as to reduce as much as possible the effect of measurement errors. For our purposes we will assume that the object (target) whose state we are estimating, and the observer (fighter) exist in a Cartesian coordinate system and that the state, S, is composed of a four- or five-element vector of the form:

$$S = \begin{bmatrix} \dot{X} \\ \dot{Y} \\ X \\ Y \end{bmatrix} \quad \text{or} \quad S = \begin{bmatrix} \dot{X} \\ \dot{Y} \\ X \\ Y \\ A \end{bmatrix} \tag{2.1}$$

where $\dot{X}$ and $\dot{Y}$ are the X and Y components of target velocity, X, Y and A are the X, Y and altitude components of target position; and where the true values of X, Y and A are assumed constant. Note that the KF in general is in no way limited to this type of reference frame or state vector, and that observations from which the estimated state is computed need not have the same dimensionality or units as the state vector. In our case, for instance, each observation will be either a bearing angle measurement or a vector of both bearing and elevation angle measurements.

The KF is a predictor-corrector type estimator that propagates an estimate, μ, of the state, S, and an associated covariance matrix, $\sum$, reflective of the accuracy of the state estimate. The KF algorithm is implemented in two alternating stages. First, previous estimates of μ and $\sum$ are extrapolated one time-step ahead based on the assumed system dynamics; this we will refer to as the Movement Step. The extrapolated quantities are then used to compute a set of optimum weights called Kalman Gains (simply proportionality factors). These are applied to the prediction and to a new observation in a Measurement Step, which provides an updated (corrected) estimate of the state and its covariance. The process is then repeated.

Symbolically, the KF algorithm may be written as follows:
Movement Step:

$$\tilde{\mu}_j = \Phi \hat{\mu}_{j-1} + \mu_w \qquad (2.2)$$

$$\tilde{\Sigma}_j = \Phi \hat{\Sigma}_{j-1} \Phi^T + Q \qquad (2.3)$$

Kalman Gain computation:

$$K_j = \tilde{\Sigma} H^T (H \tilde{\Sigma}_j H^T + P)^{-1} \qquad (2.4)$$

Measurement Step:

$$\hat{\mu}_j = \tilde{\mu}_j + K_j(Z - \mu_v - H\tilde{\mu}_j) \qquad (2.5)$$

$$\hat{\Sigma}_j = (I - K_j H)\tilde{\Sigma}_j \qquad (2.6)$$

The notation is as follows:

Φ **is the transition matrix which describes how the system state changes between observations,**

H is the transition matrix which describes how the measurement depends on the state,

μ_w, Q, μ_v, **and P are respectively, movement noise mean and covariance, and measurement noise mean and covariance. (Note that movement noise and measurement noise are assumed to be normally distributed random variables, i.e.,** $W \sim N(\mu_w, Q)$ **and** $V \sim N(\mu_v, P)$**). We will generally assume here that** μ_w, Q, **and** μ_v **are zero.**

K is the Kalman Gain,

Z is the observation (measurement),

I is the identity matrix,

j is the observation time index,

T (as superscript) indicates transpose,

~ and ^ indicate estimates after Movement and Measurement, respectively.

B. THE EXTENDED KALMAN FILTER

The above described KF is appropriate when both the movement and measurement models are linear functions of the state variables. We have, however, a non-linear measurement function since

$$Z = h(S) + V$$

where the measurement, Z, is a function, h(S), of system state plus some noise (error), V, and where h is composed of one (or two) arctangent functions of state vector elements. We have:

$$h(S) = \left[\tan^{-1} \frac{\Delta X}{\Delta Y}\right] \quad \text{in the bearing-only case, and}$$

$$h(S) = \begin{bmatrix} \tan \frac{\Delta X}{\Delta Y} \\ \tan \frac{\Delta A}{(\Delta X^2+\Delta Y^2)^{1/2}} \end{bmatrix} \quad \text{in the bearing-elevation case,}$$

where ΔX, ΔY, and ΔA are, respectively, the X, Y and altitude differences between fighter and target positions.

Since the measurement in both the bearing-only and bearing-elevation cases is a non-linear function of the

current state vector, the measurement transition matrix H in the KF algorithm must somehow be "linearized". This is accomplished by expanding h in a Taylor Series about a known vector that is close to the true state S. For this known vector we will use μ, our current estimate of S. Truncating after the first two terms of the Taylor Series we have that

$$h(S) \doteq h(\mu) + \partial h(S)/\partial S\Big|_{S=\mu}$$

The effect on the KF algorithm is that in Equation 2.5 $H\mu_j$ is replaced by the function $h(\mu_j)$ which is the measurement vector as a function of the state estimate, and in Equation 2.4 and 2.6 $H = \partial h(S)/\partial S\Big|_{S=\mu}$. One condition required here is that the estimate be unbiased, i.e., μ_v, the estimated value of V, must be zero [Ref. 3].

This extension of the KF to the non-linear case is appropriately called the Extended Kalman Filter (EKF). Higher order, more precise approximations to the optimal non-linear filter can be achieved using more terms of the Taylor Series expansion for the nonlinearities, and by deriving recursive relations for the higher moments of S. See Reference 3 for a discussion of methods of this type.

The (non-extended) Kalman Filter is optimal when its assumptions are valid [Ref. 6], however, this is not necessarily true of the EKF. Since, in our case for instance, the measurement transition matrix H both depends on the

current state estimate and is used to obtain revised state estimates, there is a potential for bad estimates to get worse and for complete loss of track to occur [Ref. 7]. Also, the matrix Σ is only an approximation to the true covariance matrix and is not always an accurate indicator of the estimation errors. Fortunately, however, the EKF has been found to perform well in a number of practical applications [Ref. 3] including passive ranging.

The design of practical, operational filters "is an art wherein one attempts to retain the behaviour of the EKF when things are going well, while simultaneously being able to recognize and correct for incipient loss of track" [Ref. 7]. Techniques for doing this (and cautions) are discussed later and in References 1, 3 and 8.

C. FUNCTIONS AND MATRICES

Functions and matrices are given here for the bearing-elevation cases. Those for the bearing-only cases are exactly the same, but excluding the last (fifth) element in the case of a vector, and the last row and column in the case of a matrix.

With μ as the estimate of the state vector $S = [\dot{X},\dot{Y},X,Y,A]^T$, we have that the movement function

$$g(S)\Big|_{S=\mu} \begin{cases} \dot{X}_i \leftarrow X_{i-1} \\ \dot{Y}_i \leftarrow Y_{i-1} \\ X_i \leftarrow X_{i-1} + \Delta t\dot{X}_{i-1} \\ Y_i \leftarrow Y_{i-1} + \Delta t\dot{Y}_{i-1} \\ A_i \leftarrow A_{i-1} \end{cases}$$

so the movement matrix is

$$\Phi = \begin{bmatrix} 1 & 0 & 0 & 0 & 0 \\ 0 & 1 & 0 & 0 & 0 \\ 1 & 0 & 1 & 0 & 0 \\ 0 & 1 & 0 & 1 & 0 \\ 0 & 0 & 0 & 0 & 1 \end{bmatrix}$$

The covariance matrix is

$$\sum = \begin{bmatrix} \sigma^2_{\dot{X}} & 0 & 0 & 0 & 0 \\ 0 & \sigma^2_{\dot{Y}} & 0 & 0 & 0 \\ 0 & 0 & \sigma^2_X & 0 & 0 \\ 0 & 0 & 0 & \sigma^2_Y & 0 \\ 0 & 0 & 0 & 0 & \sigma^2_A \end{bmatrix}$$

The measurement function is

$$h(S)\Big|_{S=\mu} = \begin{bmatrix} \tan^{-1}\left(\dfrac{\mu_X - F_X}{\mu_Y - F_Y}\right) \\ \tan^{-1}\left(\dfrac{\mu_A - F_A}{\mu_R}\right) \end{bmatrix}$$

where $\mu_R = ((\mu_X - F_X)^2 - (\mu_Y - F_Y)^2)^{1/2}$, and where F_X, F_Y, and F_A are, respectively, the fighter's known X, Y, and altitude positions, so the measurement matrix is

$$H(S)\Big|_{S=\mu} = \begin{bmatrix} 0 & 0 & \frac{\mu_Y - F_Y}{\mu_R^2} & -\frac{\mu_X - F_X}{\mu_R^2} & 0 \\ 0 & 0 & \frac{-(\mu_A - F_A)(\mu_X - F_X)}{(\mu_R^2 + (\mu_A - F_A)^2)\mu_R} & \frac{-(\mu_A - F_A)(\mu_Y - F_Y)}{(\mu_R^2 + (\mu_A - F_A)^2)\mu_R} & \frac{\mu_R}{\mu_R^2 + (\mu_A - F_A)^2} \end{bmatrix}$$

III. PARAMETERIZATION AND ASSUMPTIONS

A. FIGHTER AND TARGET FLIGHT PATHS

For all simulated tracking sessions the fighter utilizes a "zig-zag" pattern as described in Appendix B and illustrated in Figure 3.1. Briefly, this pattern has the fighter initially turn so as to have the first bearing observation 0.7 radians (about 40°) right of dead ahead, hold this heading for 1 minute, then turn to put the most recent bearing 0.7 radians left, now continuing for 2 minutes. Alternating 2-minute legs are continued until a specified number of observations have been taken, or until the target passes by the fighter. The target, meanwhile, in all cases maintains a non-turning constant altitude track. For the computer simulation runs each tracking session is limited to 5 minutes (61 observations at 5-second intervals).

B. INITIAL PARAMETERS

Eighteen different combinations of P and $\sum$ values (that is, covariances for observation error and state estimate) are utilized for initial parameterization in the simulations. The runs are first done using the "flat-Earth" motion model, then they are all repeated using the spherical-Earth model with an elevation angle correction (Appendix D), then twelve cases are simulated using the spherical-Earth model without

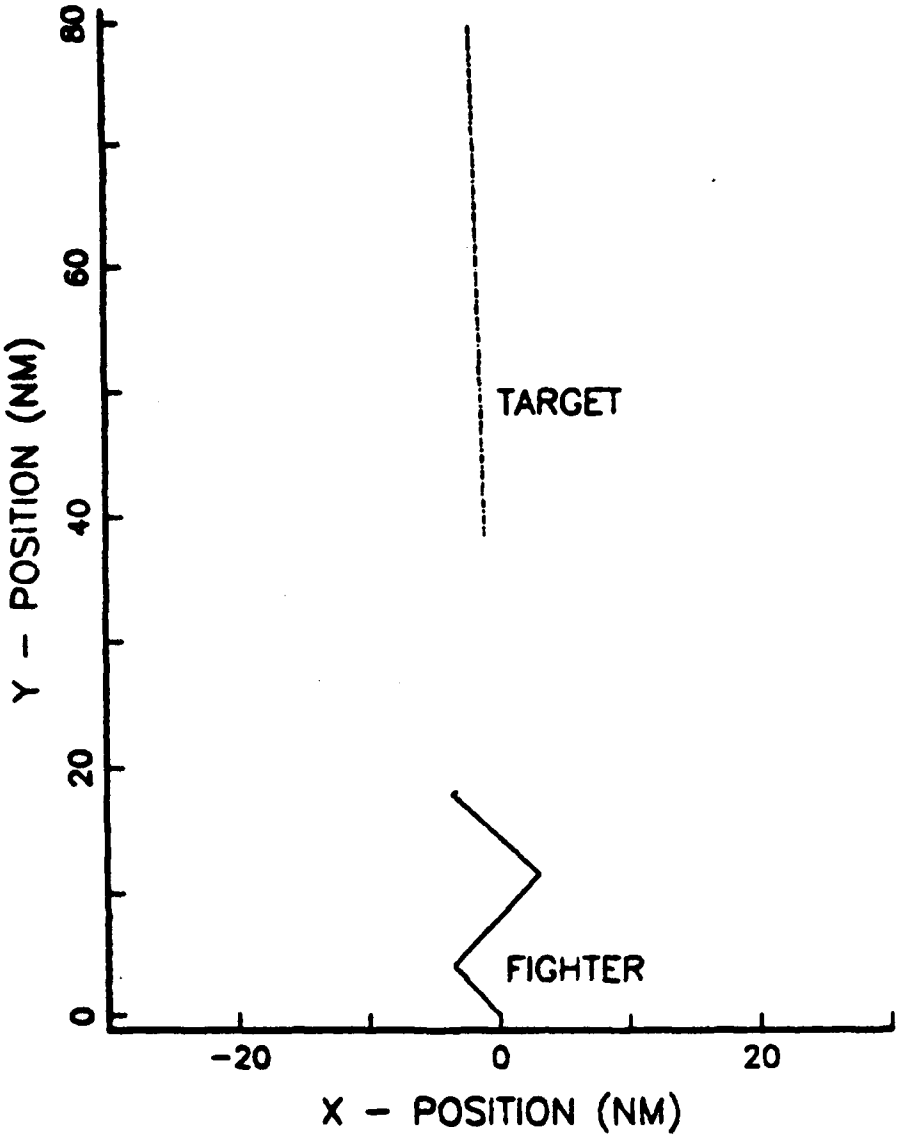

Figure 3.1. Fighter and Target Flight Paths

the elevation correction, and finally, three cases are simulated where a 5° constant bias is added to the angle measurements. 1000 replications of each set are run for both the bearing-only and bearing-elevation cases. In all cases the target, at time 0, is at 80 nautical miles (nm) range, heading directly toward the fighter at an altitude of 7nm (42,532 feet) and a ground speed of 500 knots. The fighter maintains an altitude of 3nm and a ground speed of 300 knots. The EKF initial estimates of target state for each run are varied randomly according to a multivariate normal distribution centered at the correct values, and with covariance as stated below.

At each observation the bearing-only (BO) and bearing-elevation (BE) EKF's are fed identical random azimuth measurements, while the BE EKF additionally gets random elevation angle measurements. The random measurements are generated by adding to the true angle a random number from a normal distribution with mean 0 and variance P.

The P-values used are 5^2, 2^2, 1, $.5^2$, $.1^2$, and $.02^2$ degrees^2, where these values apply to both bearing and, where applicable, elevation measurements. For example, in the first set of bearing-only simulations P = [25] whereas for the bearing-elevation runs $P = \begin{bmatrix} 25 & 0 \\ 0 & 25 \end{bmatrix}$. We assume here that both bearing and elevation measurements have the same magnitude and distribution of errors (normal), and that they are independent of each other.

The initial estimate of the covariance matrix has diagonal values: $\sigma^2_{\dot{X}} = 1000$ knots^2, $\sigma^2_{\dot{Y}} = 250{,}000$ knots^2, $\sigma^2_X = 4$nm^2, and $\sigma^2_A = 4$nm^2, while σ^2_Y is varied from 1600nm^2 to 400nm^2 to 100nm^2 for the different cases. The choices for these values as well as for the P-values are somewhat arbitrary and their validity will not be argued here. The reader is referred to Appendix B for a description of how the reference frames (coordinate systems) are defined, and of how true positions and observation angles are computed.

C. ASSUMPTIONS

For EKF computer simulations the following assumptions are made:

(1) The observer (fighter) knows his own position, course and speed precisely.

(2) Maneuvers are instantaneous; there is neither time loss nor positional change associated with the observer's course changes.

(3) The target holds a constant course, speed and altitude, while the fighter holds constant speed and altitude.

(4) There is no refraction or other distortion of the radiated energy.

(5) Angle measurement errors in elevation and in azimuth have a Gaussian (normal) distribution with zero mean and known variance. Errors are assumed to be independent of range.

IV. SIMULATION RESULTS AND OBSERVATIONS

A. TABLES

Results of the computer simulations are summarized in Tables I-IV which are for, respectively, the planar ("flat-Earth") motion model, the spherical-Earth motion model with elevation angle correction, the spherical model without elevation angle correction, and, finally, the spherical model with elevation angle correction, but with a constant angle bias inserted into the observations. Data in the tables are categorized by initial range variance, and for each range variance the different selections of angle measurement precision are represented, with data from the bearing-only EKF on the left and from the bearing-elevation EKF on the right.

Comparison data are the proportions of dropped tracks using three different criteria. First is the "$\varepsilon > 3\sigma$" column, which lists the proportion of runs in which actual range error was greater than the 3 standard deviations as estimated by the EKF, i.e., $\varepsilon = |R-\hat{R}| > 3\sigma$. (See Appendix A for a description of computations of R and σ_R^2.) The "Rg" column lists as dropped tracks those for which the final range estimate is in error by more than 25% of the true range, and the "Rg-Vel" column lists those for which either range or velocity are in error by more than 25% of actual values.

TABLE I

Simulation Results--"Flat-Earth" Motion Model

Proportion of Dropped Tracks
(by criterion)

1000 Replications

Bearing-only				Bearing & Elevation		
Initial Range Variance = $\sum(4,4) = 40^2 nm^2$						
			P Degrees^2 Measurement Precision			
$\varepsilon > 3\sigma$	Rg-Vel	Rg		$\varepsilon > 3\sigma$	Rg-Vel	Rg
0.188	0.949	0.732	5^2	0.075	0.880	0.554
0.085	0.757	0.452	2^2	0.047	0.473	0.169
0.094	0.480	0.175	1_2	0.073	0.206	0.059
0.124	0.235	0.109	$.5^2$	0.118	0.137	0.076
0.217	0.179	0.128	$.1^2$	0.208	0.153	0.092
0.387	0.177	0.138	$.02^2$	0.439	0.168	0.096
$\sum (4,4) = 20^2 nm^2$						
$\varepsilon > 3\sigma$	Rg-Vel	Rg	P	$\varepsilon > 3\sigma$	Rg-Vel	Rg
0.121	0.904	0.710	5^2	0.042	0.781	0.504
0.017	0.664	0.329	2^2	0.004	0.347	0.096
0.006	0.328	0.050	1_2	0.004	0.038	0.001
0.010	0.083	0.001	$.5^2$	0.006	0.009	0.001
0.066	0.029	0.007	$.1^2$	0.041	0.016	0.003
0.241	0.029	0.007	$.02^2$	0.184	0.012	0.001
$\sum (4,4) = 10^2 nm^2$						
$\varepsilon > 3\sigma$	Rg-Vel	Rg	P	$\varepsilon > 3\sigma$	Rg-Vel	Rg
0.131	0.858	0.713	5^2	0.032	0.701	0.484
0.017	0.501	0.293	2^2	0.002	0.203	0.071
0.011	0.239	0.030	1_2	0.001	0.018	0.000
0.003	0.039	0.000	$.5^2$	0.004	0.000	0.000
0.014	0.002	0.000	$.1^2$	0.006	0.000	0.000
0.107	0.001	0.000	$.02^2$	0.037	0.000	0.000

B. OBSERVATIONS

Some immediate observations can be made from the tables:

1. From Table I ("flat-Earth" Motion Model), the bearing-elevation results appear superior to those for bearing-only for every set of parameters when using either the range-velocity or range error criteria, and they are generally superior when using the $\varepsilon > 3\sigma$ criterion as well. It should be noted, however, that in all of the cases represented the fighter-target altitude difference is held at 4nm (about 24,000 ft). The advantage of BE over BO was shown by limited additional simulations to disappear as the altitude difference went to zero.

2. Improvement in the accuracy of the initial range estimate (decrease in the variance $\sum(4,4)$) from 40^2 to 20^2, and then to $10^2 nm^2$ has a positive effect in decreasing the proportion of dropped tracks as one might reasonably expect.

3. Improvement in angle measurement precision (variance P) generally improves the EKF's ability to track. It seems evident, for instance, that $P = 5^2$ is impractical from an operational standpoint since neither EKF could determine target range and velocity within 25%, even 30% of the time regardless of initial range variance. It is interesting to note that the $\varepsilon > 3\sigma$ dropped track criterion for the BE EKF for $P = 5^2$ is exceeded in a much lower (2-10%) proportion of the cases than are the range and range-velocity standards (50-95%). This is a valuable trait in that, although the

TABLE II

Simulation Results--Spherical Motion Model
with Elevation Correction

Proportion of Dropped Tracks
(by criterion)

1000 Replications

Initial Range Variance = $\sum(4,4) = 40^2 nm^2$

Bearing-only			P Degrees^2 Measurement Precision	Bearing & Elevation		
$\varepsilon>3\sigma$	Rg-Vel	Rg		$\varepsilon>3\sigma$	Rg-Vel	Rg
0.255	0.937	0.751	5_2^2	0.121	0.878	0.592
0.082	0.718	0.370	2^2	0.073	0.466	0.195
0.076	0.458	0.145	1_2	0.085	0.159	0.049
0.125	0.224	0.106	$.5_2^2$	0.160	0.139	0.075
0.231	0.178	0.120	$.1^2$	0.440	0.179	0.111
0.393	0.170	0.129	$.02^2$	0.858	0.262	0.174

$\sum (4,4) = 20^2 nm^2$

$\varepsilon>3\sigma$	Rg-Vel	Rg	P	$\varepsilon>3\sigma$	Rg-Vel	Rg
0.238	0.919	0.752	5_2^2	0.122	0.808	0.542
0.027	0.626	0.252	2^2	0.010	0.291	0.078
0.013	0.350	0.049	1_2	0.012	0.043	0.004
0.018	0.084	0.007	$.5_2^2$	0.034	0.013	0.003
0.065	0.027	0.008	$.1^2$	0.247	0.012	0.006
0.221	0.028	0.006	$.02^2$	0.801	0.078	0.045

$\sum (4,4) = 10^2 nm^2$

$\varepsilon>3\sigma$	Rg-Vel	Rg	P	$\varepsilon>3\sigma$	Rg-Vel	Rg
0.238	0.842	0.721	5_2^2	0.083	0.663	0.478
0.024	0.478	0.233	2^2	0.003	0.203	0.066
0.004	0.219	0.023	1_2	0.005	0.015	0.000
0.003	0.047	0.000	$.5_2^2$	0.006	0.000	0.000
0.012	0.001	0.000	$.1^2$	0.142	0.000	0.000
0.088	0.000	0.000	$.02^2$	0.742	0.059	0.050

EKF estimates of target state are not very accurate, the EKF is apparently "aware" of this since its estimated range variance is evidently high. Since the state covariance matrix is available to the user, he should generally be able to determine the worth of the estimated state information.

4. This characteristic does not necessarily hold true when measurement precision is extremely high, however; in fact, it becomes less true as P-values are decreased below $.5^2$ for these EKF's (e.g., Table I, $\sum(4,4) = 40^2$ and $P = .02^2$). A similar observation was made in Reference 6. This apparent EKF trait may be explained by the Taylor Series approximation used to linearize the Measurement Function (Chapter II) inducing more error than that added by the noisiness of the bearing measurements. The EKF-estimated range variance becomes relatively small because of the precise measurements, but the actual range errors are not correspondingly reduced apparently because of the EKF linearization approximation. Practical results are still quite good as evidenced by the still relatively small proportion of dropped tracks using the range and range-velocity criteria. With a longer observation period, however, we might expect the estimated range variance to continue its decrease relative to the squared range error (covariance collapse), and we would anticipate more tracks being dropped. A possible solution to this problem, if highly precise angle measurements are

TABLE III

Simulation Results--Spherical Motion Model
Without Elevation Correction

Proportion of Dropped Tracks
(by criterion)

1000 Replications

Bearing-only				Bearing & Elevation		
			Initial Range Variance = $\sum (4,4) = 40^2 nm^2$			
			P Degrees^2 Measurement Precision			
$\varepsilon > 3\sigma$	Rg-Vel	Rg		$\varepsilon > 3\sigma$	Rg-Vel	Rg
0.079	0.726	0.356	2^2	0.079	0.477	0.126
0.071	0.420	0.127	1	0.137	0.239	0.055
0.108	0.205	0.090	$.5^2$	0.372	0.130	0.071
0.219	0.017	0.129	$.1^2$	0.998	0.166	0.117
			$\sum (4,4) = 20^2 nm^2$			
$\varepsilon > 3\sigma$	Rg-Vel	Rg	P	$\varepsilon > 3\sigma$	Rg-Vel	Rg
0.035	0.609	0.254	2^2	0.028	0.336	0.044
0.069	0.156	0.002	1	0.069	0.156	0.002
0.011	0.073	0.006	$.5^2$	0.312	0.022	0.002
0.053	0.017	0.002	$.1^2$	1.000	0.005	0.002
			$\sum (4,4) = 10^2 nm^2$			
$\varepsilon > 3\sigma$	Rg-Vel	Rg	P	$\varepsilon > 3\sigma$	Rg-Vel	Rg
0.023	0.502	0.237	2^2	0.027	0.226	0.050
0.002	0.222	0.017	1	0.065	0.098	0.000
0.006	0.041	0.000	$.5^2$	0.328	0.019	0.000
0.008	0.001	0.000	$.1^2$	1.000	0.000	0.000

TABLE IV

Simulation Results--Spherical Motion Model
with Measurement Bias

Proportion of Dropped Tracks
(by criterion)

1000 Replications

Bearing-only					Bearing & Elevation		
			Az Bias	Elev Bias			
$\varepsilon>3\sigma$	Rg-Vel	Rg			$\varepsilon>3\sigma$	Rg-Vel	Rg
0.132	0.238	0.113	0	5	0.520	0.838	0.235
0.991	0.999	0.989	5	0	0.865	0.951	0.759
0.985	0.999	0.986	5	5	0.747	0.998	0.749

Initial Range VAriance = $\sum (4,4) = 40^2 nm^2$

Measurement Precision = $P = .5^2$

available, would be to use a higher order Taylor Series approximation as previously suggested.

5. A comparison of Tables I and II indicates that spherical motion target data can be accommodated by the flat-Earth EKF when an appropriate elevation angle correction is applied. At the very high precision levels, however, there is a notable degradation with the BE EKF results, especially when using the $\varepsilon > 3\sigma$ criterion. This is apparently due to the filter being "confused" by highly accurate measurements which are "corrected" by an elevation angle correction (for Earth's curvature) which is no longer

adequate. The result is that estimated range variance is considerably smaller than actual range variance.

6. A comparison of Tables II and III indicates that the BE EKF is somewhat improved when using the elevation angle correction to allow for the Earth's curvature, but the filter without the correction still performs almost as effectively. (The BO EKF, of course, is not affected by the correction since it does not use elevation angle as an input). As angle measurement precision increases, the positive effect of an elevation angle correction to the BE EKF also increases, however (e.g., Tables I and II, $\sum(4,4) = 40^2$, $P = .1^2$).

7. Table IV illustrates the effects of biased measurement data on EKF performance. When azimuth angle, or both azimuth and elevation angles have a bias, then neither filter operates effectively. When only the elevation angle is biased the BE EKF performance is severely degraded. Only the $P = .25$ measurement precision was investigated; it was felt to be a good test case since it consistently produced among the best results with unbiased inputs.

C. TIME SEQUENCE PLOTS

Figure 4.1 is a set of plots showing a time sequence of range errors during the 5 minutes of tracking. The median values of range errors are represented for the 1000 replications of each of the different levels of measurement precision (P). A representative set of plots are shown in

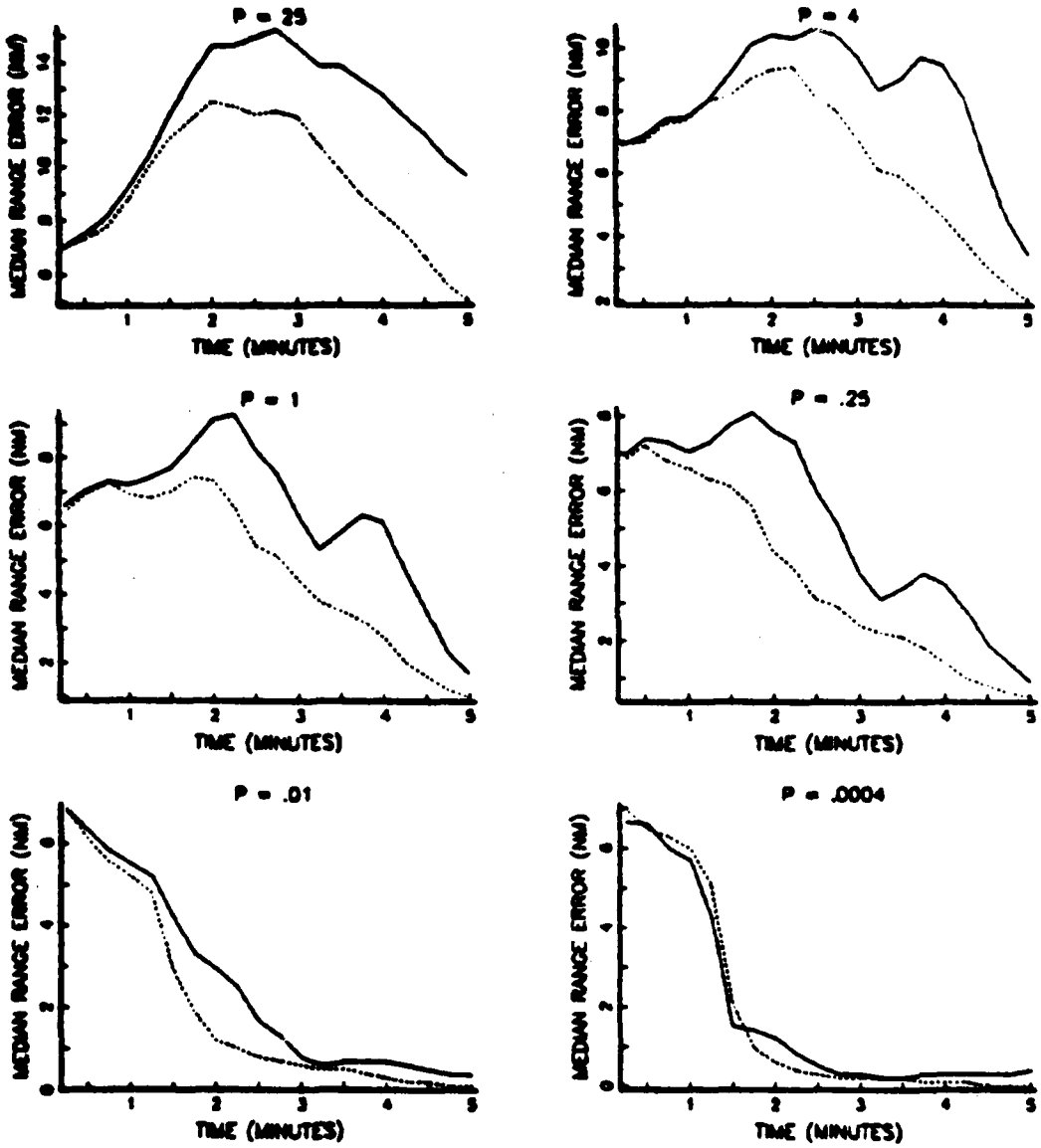

Figure 4.1. Median Range Error Vs. Time--"Flat-Earth" Model, Range Variance = $100nm^2$

Figure 4.1 which are for the "flat-Earth" motion model with range variance of $100nm^2$. Similar plots for the other sets of parameters are included at the end of the chapter. Note that the horizontal axis is not always at zero range error, and that the vertical scales differ among plots. In each plot the solid line represents BO EKF results, whereas the dotted line represents those from the BE EKF.

Several important features of the EKF's are illustrated by the plots:

1. The BE EKF is again seen to be generally superior to the BO EKF. The major advantage of the BE EKF seems to be the generally greater speed with which the estimated range converges to true range particularly in the lower measurement precision cases. At very fine measurement precision ($P = .01$ and $P = .0004$ degrees^2) there seems to be little if any advantage to using both bearing and elevation angles.

2. In all cases the trend seems to be toward better convergence with time, once the initial transients have disappeared. This suggests that even in those cases where a large proportion of the runs are "dropped tracks" according to the range or range-velocity criterion, additional tracking time, if available, would bring increasing numbers into convergence. Limited additional computer simulations seemed to bear this out.

3. The "humps" which are especially prominent in the $P = 2^2$, 1, and $.5^2$ cases occur at about 2 and 4 minutes.

They indicate that range error is decreasing from time 0 to 1, increasing from time 1 to 2, decreasing again from 2 to 3, etc. Referring to Figure 3.1 (Fighter and Target Flight Paths) the convergence of estimated range to true range, then, appears to increase as the rate of bearing change increases. This is consistent with the well known (among submariners) result that in passive ranging "the greater the time rate of change of bearing the more accurate the range estimate" [Ref. 9]. This rate is slowest (with this particular geometry) when the fighter first turns in toward target flight path, increasing until he next turns in from the opposite side of target flight path. The humps, then, roughly coincide with the times at which the fighter is turning back in, i.e., the times when bearing change rate is relatively low.

4. It is evident that the time to convergence is greatly affected by angle measurement precision. Note that in the $P = .02^2$ case convergence is extremely rapid after 1 minute, which is the time of the first fighter turn. This suggests that in the case of extremely good precision, convergence time can be even further decreased by making the fighter's first turn earlier, or perhaps having the fighter maintain a constantly turning flight path such as the "sine wave" flight path proposed by Ohlmeyer [Ref. 1]. Limited additional simulations with the fine precision and an earlier turn did, in fact, indicate that convergence time would be reduced.

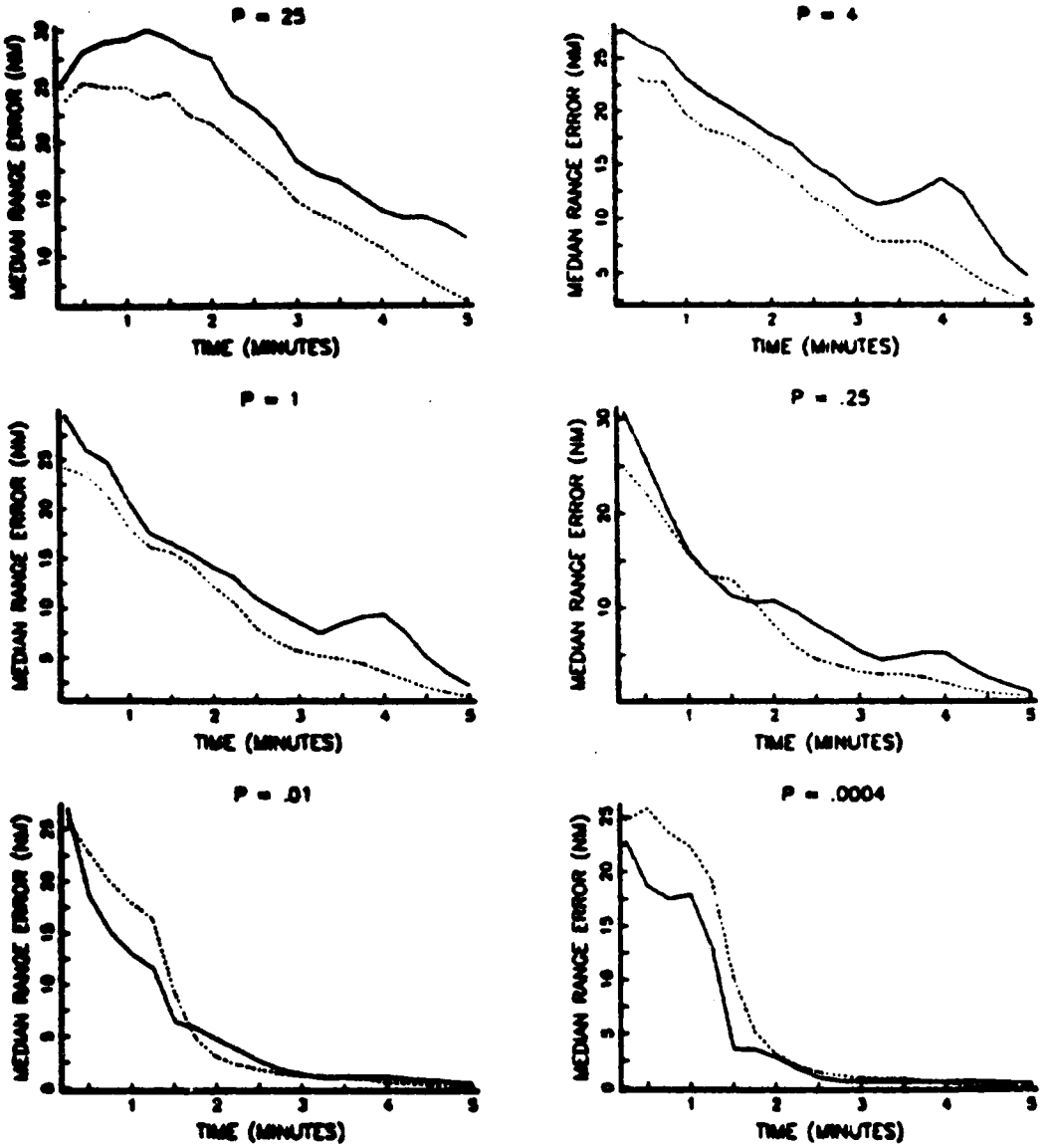

Figure 4.2. Median Range Error Vs. Time--"Flat-Earth" Model, Range Variance = 1600nm^2

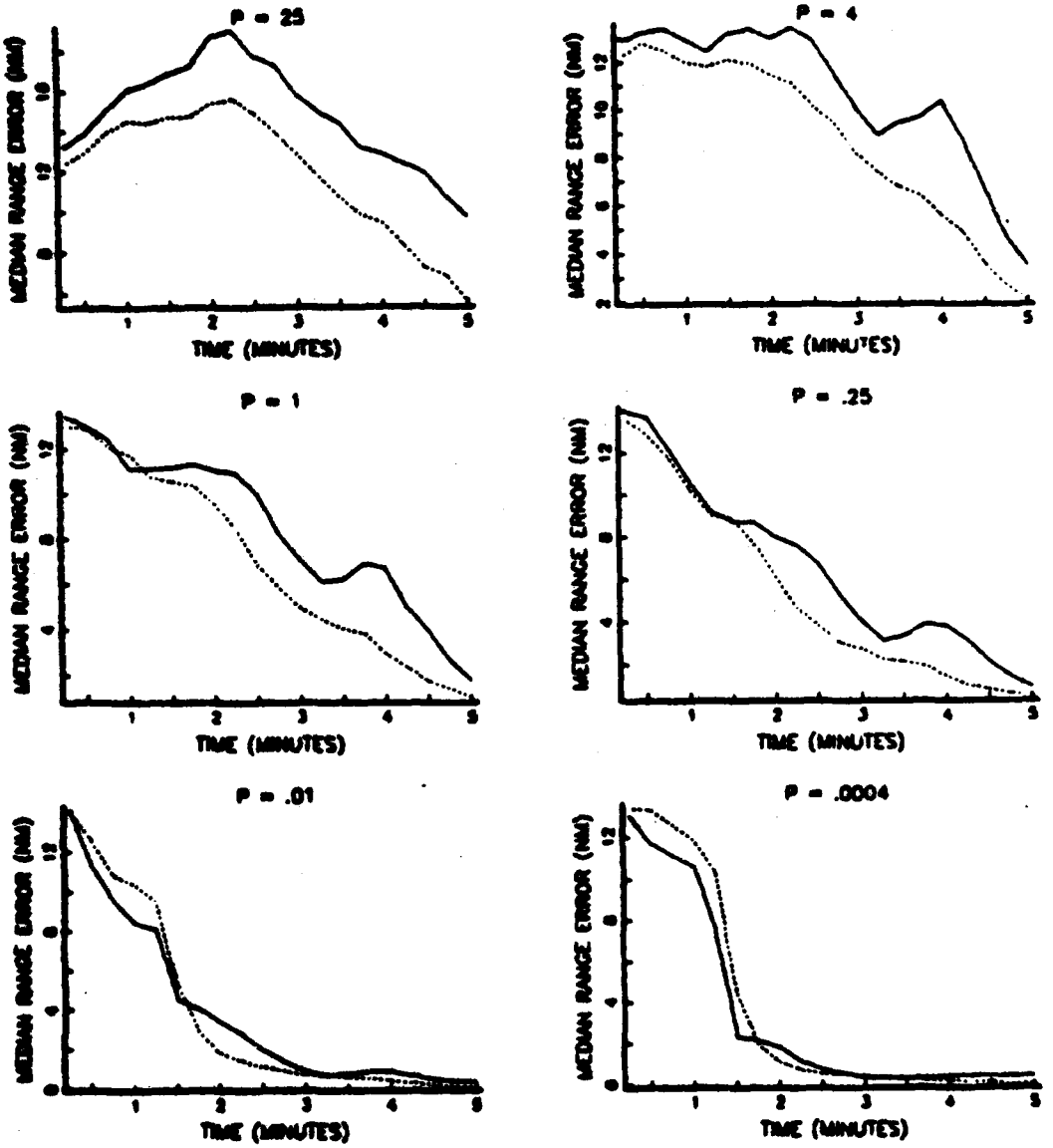

Figure 4.3. Median Range Error Vs. Time--"Flat-Earth" Model, Range Variance = 400nm^2

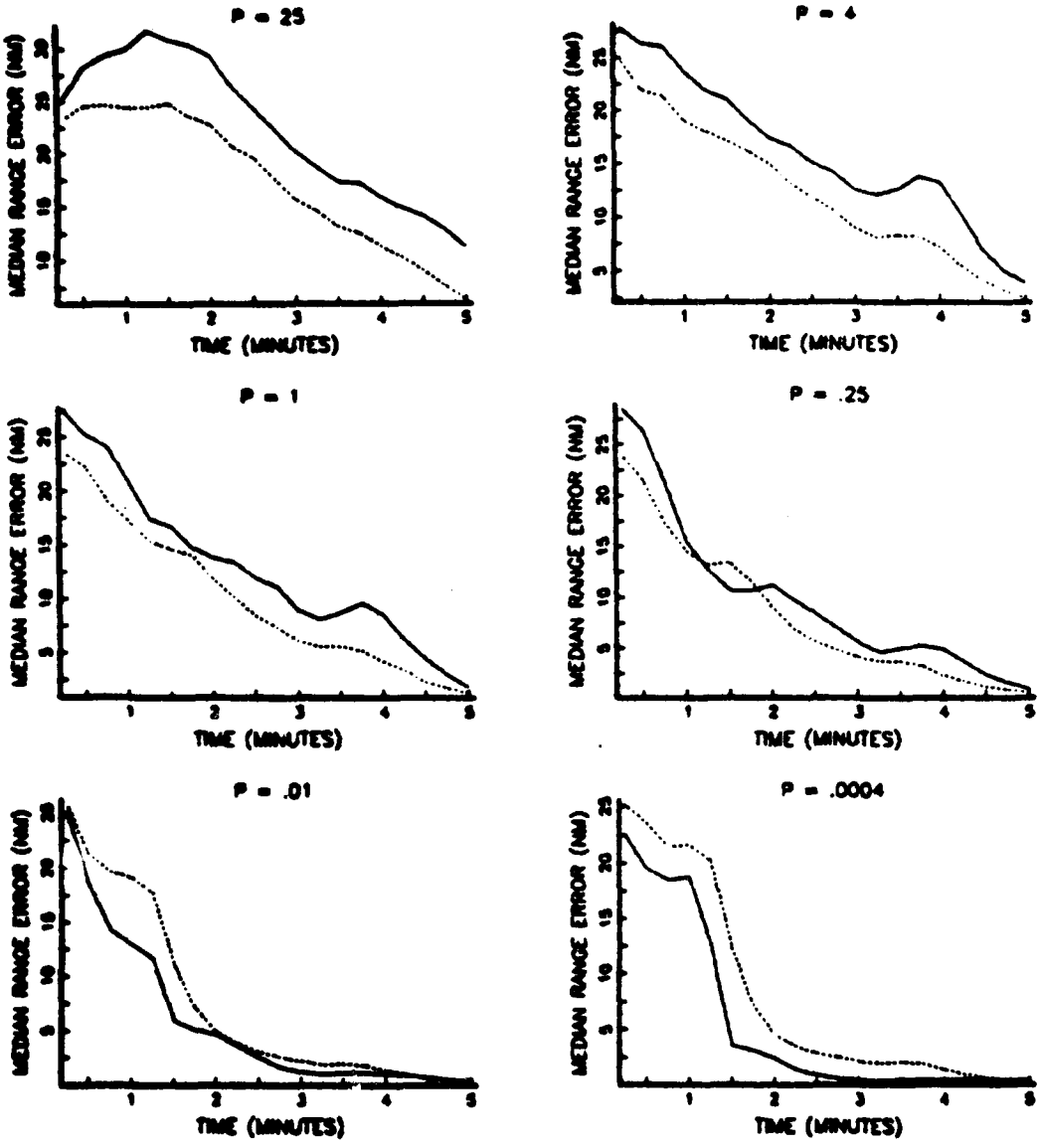

Figure 4.4. Median Range Error Vs. Time-Spherical Model, Range Variance = 1600nm^2

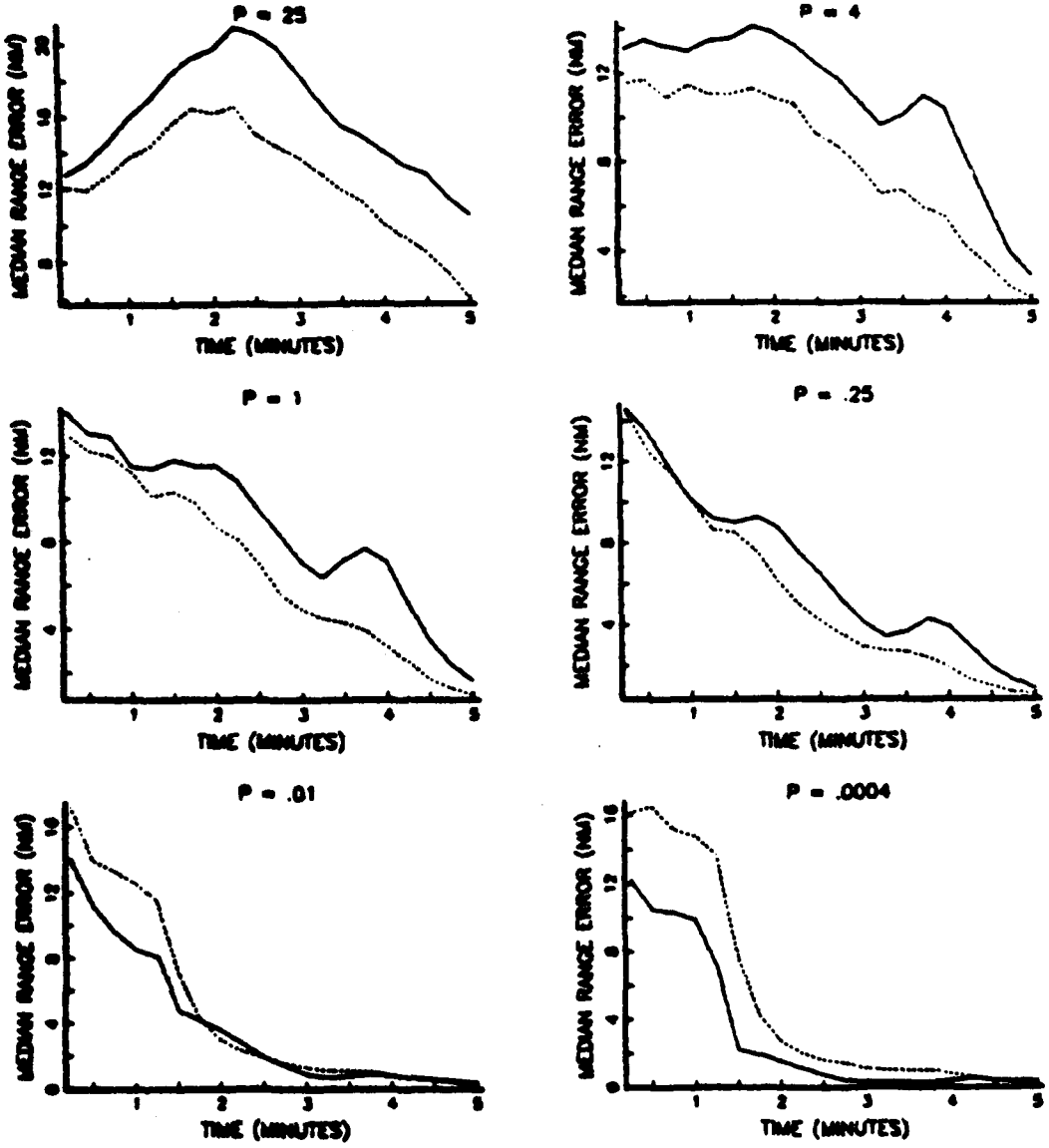

Figure 4.5. Median Range Error Vs. Time--Spherical Model, Range Variance = 400nm^2

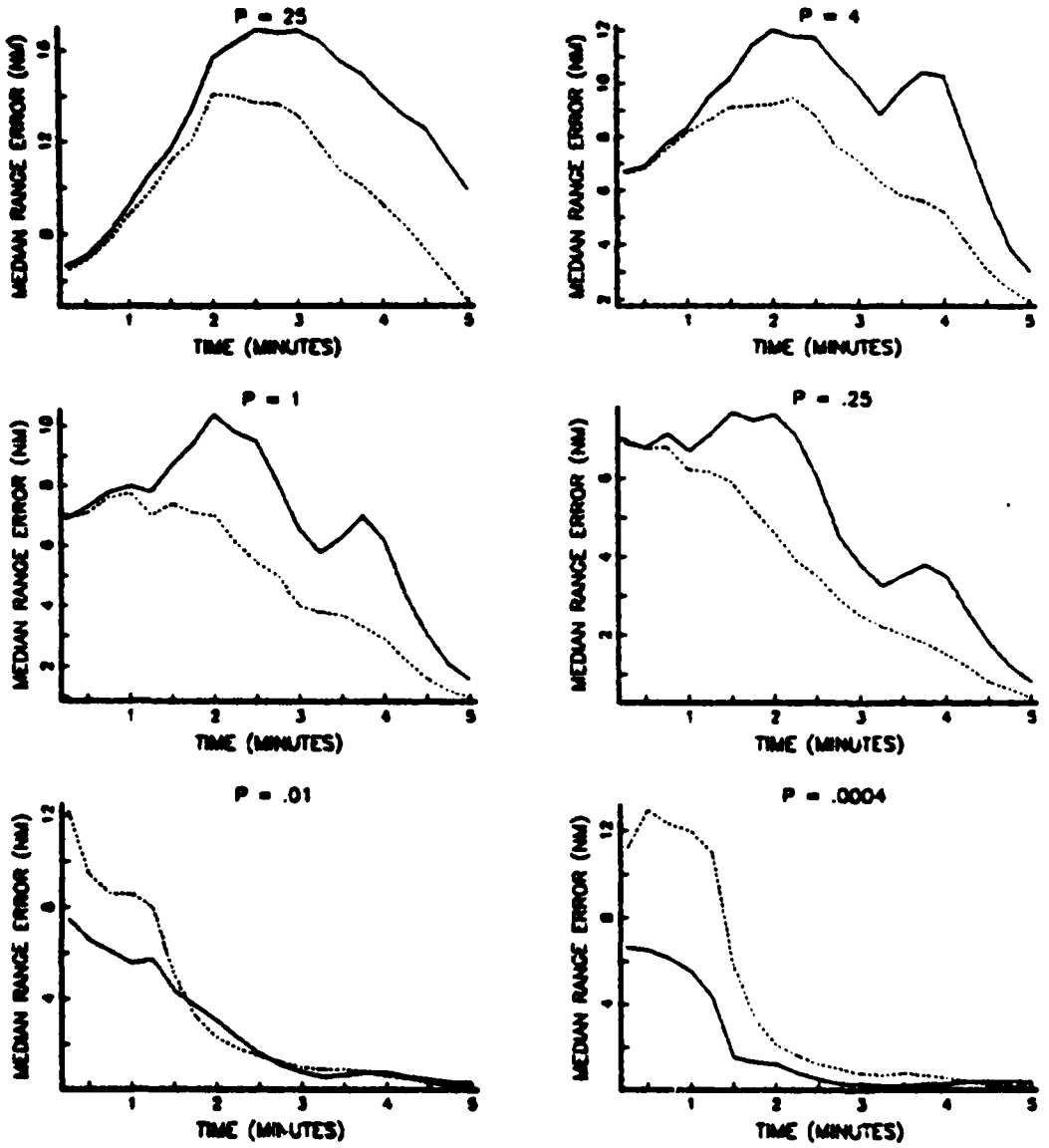

Figure 4.6. Median Range Error Vs. Time--Spherical Model, Range Variance = 100nm^2

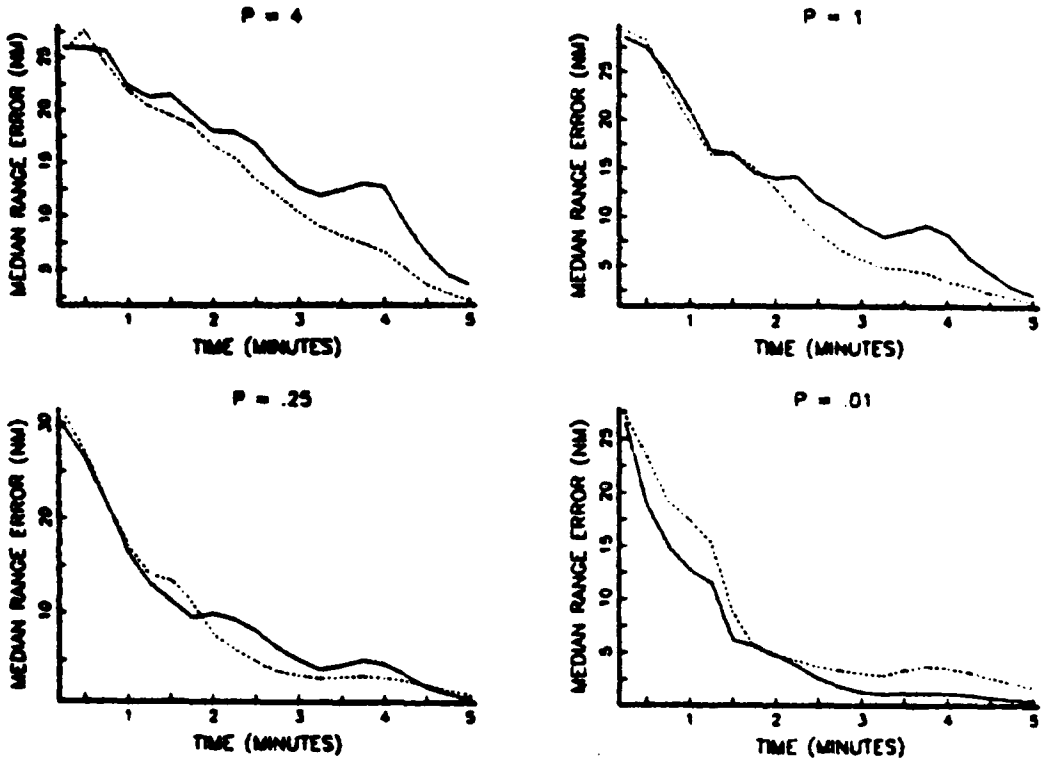

Figure 4.7. Median Range Error Vs. Time--Spherical Model (No Elev. Correction), Range Variance = 1600nm^2

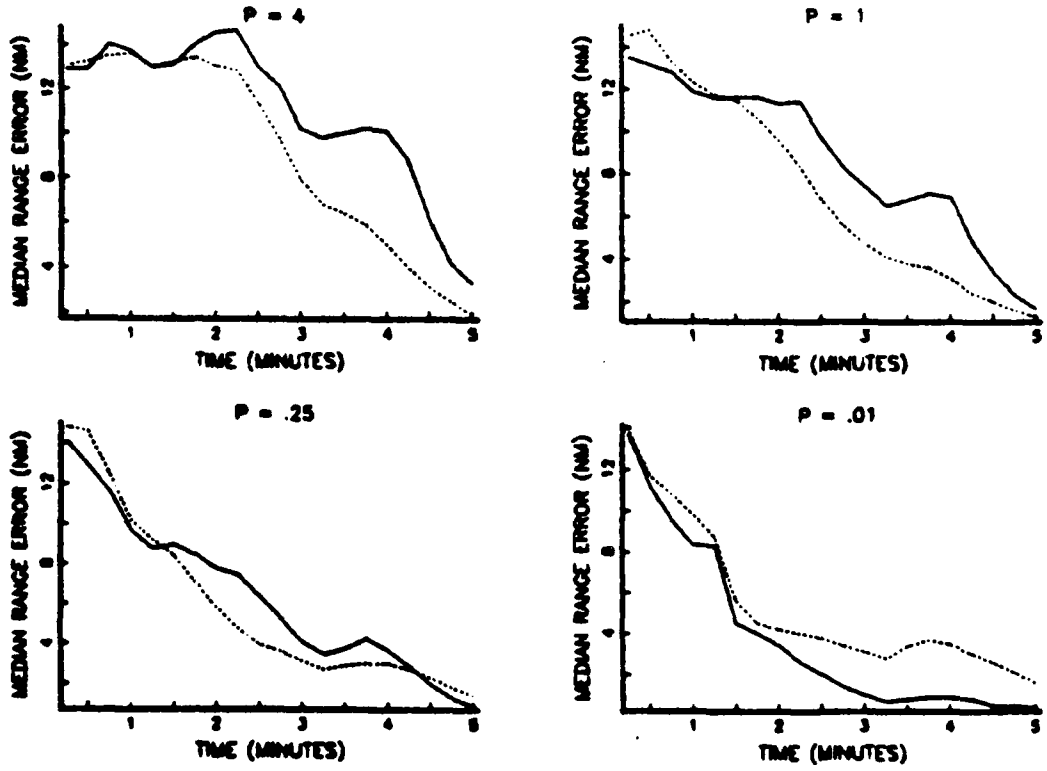

Figure 4.8. Median Range Error Vs. Time--Spherical Model (No Elev. Correction), Range Variance = 400nm^2

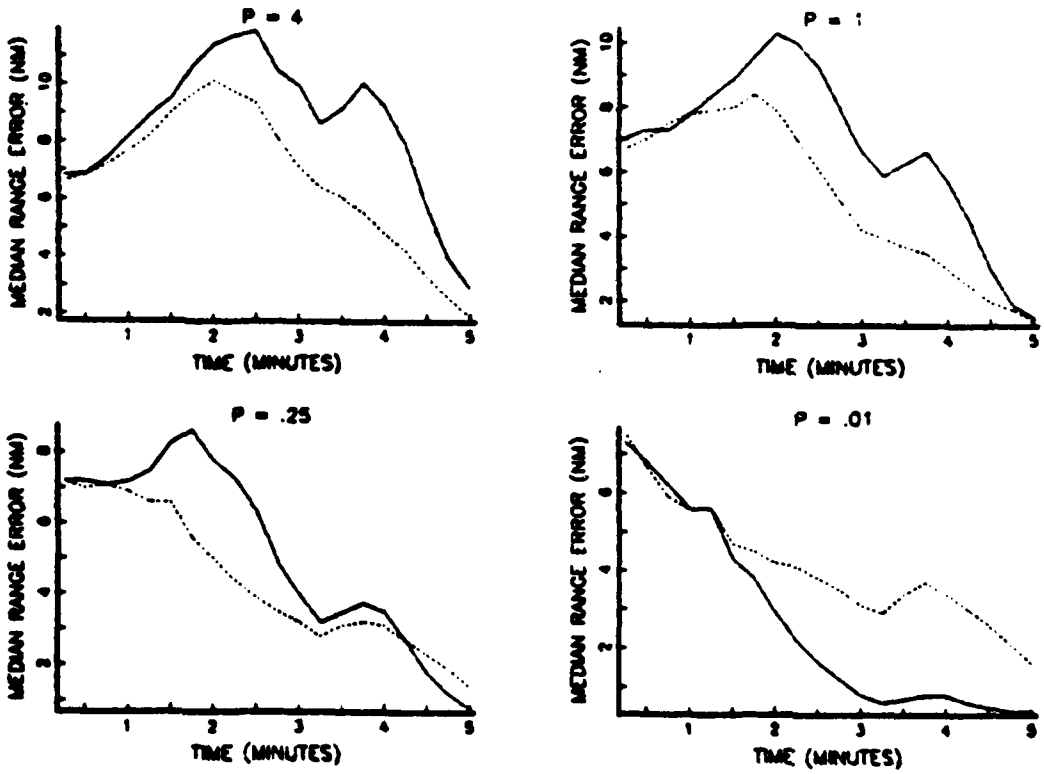

Figure 4.9. Median Range Error Vs. Time--Spherical Model (No Elev. Correction), Range Variance = $100nm^2$

V. CONCLUSIONS AND RECOMMENDATIONS

A. CONCLUSIONS

Computer simulations using the two EKF algorithms presented here demonstrate that both have the potential to be valuable tools for air-to-air passive ranging as long as their assumptions are met. The bearing-elevation EKF generally performs better than the bearing-only EKF when the fighter and target have a significant separation in altitude.

B. RECOMMENDATIONS

There are several possible EKF modifications which seem to offer potential in improving its performance. Some of these are:

1. Filter re-initialization when it is determined to be grossly in error. Aidala [Ref. 8], discusses ways in which "premature covariance collapse" can be recognized. He notes that onset of this malady, which usually leads to a dropped track, often occurs after only two initial measurements. This suggests that if it can be recognized there would normally be ample time to restart the EKF. He also cautions that some "previous attempts to prevent abnormal filter behavior have proved ineffectual when subjected to rigorous testing...because they focus only on

the symptoms of the problem (rather than) the underlying causes" [Ref. 8].

2. Filter self-correction when obtaining "unbelievable" results. Although this may fall into the category of treating the "symptom" rather than the ailment, it seems reasonable to put some bounds on the acceptable estimated target state based on physical knowledge. The most obvious limit would apply to a low target; for example a fighter at an altitude of 3nm with a target elevation observation of -4° could immediately deduce that the target is (depending on measurement precision) no farther away from him than $R \leq 3 \csc 4° = 43$nm, since he can generally be assumed to be above the Earth's surface, so it would seem futile to waste more time estimating him at, say, 80nm. Similarly, the maximum altitude of a target may be known, as well as possible limits on speeds, ranges, or headings. These things would be scenario-dependent and would probably require aircrew inputs and reasonable default values.

3. Increased frequency of observations (filter cycle rate). A five-second interval was chosen for these simulations because that seemed long enough to ensure independence among measurements in an operational system, and because it reduced the computer time required to do the many replications. A few simulations using three-second and one-second intervals obtained slightly faster convergence though little improvement in the numbers of dropped tracks.

4. Optimized fighter PR maneuver. Since the rate of convergence to the true target state evidently increases with the rate of bearing angle change, this should be considered in choosing fighter maneuvers. A pure collision course is not conducive to good passive ranging, especially for the BO EKF, since it precipitates no bearing change, but an alternating lead-lag, for instance, may accomplish virtually the same thing tactically, yet allow sufficient bearing change for a PR solution. The "optimum" maneuver would undoubtedly be different for varying scenarios and equipments. Altitude and speed changes as well as horizontal turns should be considered. The APL program (Appendix E) used to model these EKF's can be easily modified to accommodate different fighter and target flight paths, and so could be a useful tool in comparing PR maneuvers.

5. P-values (observation precision) adjusted to actual equipment specifications. This may entail varying the P-values as a function of range. Simulation results using this change are shown in Reference 1. Other equipment-peculiar characteristics such as own-ship navigation error would also have to be considered. For these simulations it was assumed that the distribution of angle measurement errors was known. The effects of giving the EKF wrong precision error distribution information should be investigated.

6. Interactive system. The aircrewman may have a variety of sources of a priori information with which to

make an initial or updated estimate of target state. There should be a means for him to insert this information along with a confidence level or estimated variance, and, as mentioned above, there should be a set of reasonable default values.

7. Measurement variance reduction. For example, several measurements could perhaps be averaged to obtain one observation input which is less affected by individual outliers. This could be particularly important for the first few observations, since as Aidala [Ref. 8] suggests, they are so influential in the "premature covariance collapse" problem.

8. Maneuvering target recognition and tracking. This continues to be an unsolved problem. Ohlmeyer [Ref. 1], suggests "that small levels of target acceleration can be accommodated within the filter (using methods such as) the introduction of state process noise."

9. Parallel filters. If computer capacity is available, it may be advantageous to have more than one EKF operating at the same time on the same target. The separate filters might use alternating observation inputs, or perhaps initialize at different times. Besides rendering a "second opinion" this could be helpful in the maneuvering target situation.

10. Multiple target processing. Since fighter maneuvers need not generally be precisely designed for a specific target, the fighter could be making his maneuvers against

a particular, perhaps primary, target, and concurrently be computing passive ranging solutions on other targets if his equipment has sufficient sensor capability and computer capacity.

11. Elevation angle-only EKF. There could be situations for which the fighter would want to maintain a collision course in azimuth (precluding bearings-only passive ranging) and yet desire a PR solution. This could conceivably be accomplished with altitude changes and an EKF which requires only elevation angle observations.

APPENDIX A

VALIDATION

A. VALIDATION METHOD

The method of validation used here is borrowed from Daly [Ref. 6]. In essence, validity is claimed if the EKF tracks in range variance as well as in range.

If the EKF is operating properly and if it is being provided with accurate enough information, then the estimates of range variance after individual tracking sessions should be very close to the true range variance. Comparisons of the EKF variance estimates over many tracking sessions with the actual (sample) variances provide a means of evaluating the consistency of the EKF range estimates. As a measure of this consistency we will use the statistic K1 which is the ratio of sample range variance to EKF-estimated range variance at the end of a tracking session, averaged over n distinct sessions.

$$K1 = \frac{1}{n} \sum_{i=1}^{n} \left(\frac{(R_i - \hat{R}_i)^2}{\sigma^2_{R_i}} \right)$$

$\hat{R}_i$ is the EKF range estimate, R_i is the true range, and $\sigma^2_{R_i}$ is the EKF range variance estimate, all at the end of tracking session i. The tracking session is simulated

n = 1000 times using the same values for all input parameters, but using distinct random number streams for measurement errors and initial state estimate errors. The method for computing R and σ_R^2 is described below in Section C.

We expect that if our theory is correct and the EKF has accurately estimated the true range variance, that the value of K1 will tend toward unity.

The EKF algorithms were applied to the same passive ranging problem (scenario) which was addressed in Reference 6. In this problem the observer and target are both surface ships. At time 0 the target bears 090° at 20nm. The target proceeds on a course of 360° at 10 kts, while the observer,

TABLE V

K1 Values--Surface Ship Scenario

Flat-Earth Motion Model

1000 Replications

P	$\sum(4,4) = 10^2$	$\sum(4,4) = 1$
10^1	0.982	1.015
10^0	0.957	0.015
10^{-1}	0.991	0.953
10^{-2}	0.985	0.959
10^{-3}	0.947	0.976
10^{-4}	1.048	0.955
10^{-5}	1.075	1.091
10^{-6}	1.140	1.086
10^{-7}	3.750	0.941
10^{-8}	7.461	3.348

for his passive ranging maneuver, proceeds on a course of 180° for 15 minutes, then turns (instantaneously) to a course of 360° for another 15 minutes. A total of 11 observations are taken at 3 minute intervals.

B. VALIDATION RESULTS

Table V illustrates that the K1 values do indeed generally tend toward unity, thus supporting our claim of validity. It is notable that with extremely fine measurement precision the K1 values no longer stay near 1. This finding was also reported in Reference 6. As discussed in Chapter IV, this seems to be a result of the range variance decreasing because of the fine precision, whereas the actual range errors are apparently limited in their decrease by the errors inherent in the EKF due to its linearization approximation in the Measurement Step.

Results in Reference 6 were obtained using an EKF parameterized with range, bearing, velocity, and direction, rather than X, Y, X-velocity, and Y-velocity as used here. The author reports that he had obtained similar results using the latter parameterization, but that when using the $(\dot{X},\dot{Y},X,Y)$ parameterization the K1 values stayed close to 1 for a higher degree of measurement precision. Results contained here appear to confirm that.

When this same technique was applied to the scenario described in Chapter III the resulting K1 values were less clearly convergent to 1 (Table VI). While being somewhat

TABLE VI

Kl Values--Fighter Scenario

Flat-Earth Motion Model

1000 Replications

Bearing-Only

P	$\sum(4,4) = 40^2$	$\sum(4,4) = 20^2$	$\sum(4,4) = 10^2$
5^2	0.981	0.893	0.897
2^2	0.932	0.882	0.873
1	0.904	0.868	0.835
$.5^2$	0.853	0.840	0.833
$.1^2$	0.851	0.799	0.834
$.02^2$	0.938	0.843	0.826

Bearing & Elevation

P	$\sum(4,4) = 40^2$	$\sum(4,4) = 20^2$	$\sum(4,4) = 10^2$
5^2	1.090	0.964	0.900
2^2	0.893	0.846	0.832
1^2	0.839	0.826	0.837
$.5^2$	0.831	0.801	0.774
$.1^2$	0.889	0.816	0.823
$.02^2$	1.146	0.983	0.829

"close" to 1 (±0.2) the Kl values varied from 1 significantly more than those for the simpler problem (±0.05). Only those values which were less than 10 were included in this computation of the average Kl's; this was done to eliminate the effect of those (normally few) dropped track Kl values which diverged drastically from 1, e.g., 10^6,

due to the much larger number of iterations per tracking session. This limit was picked arbitrarily and may partially account for most of the average Kl's being less than 1. The variation in the values seems to infer that the rate of convergence is scenario-dependent in that it is affected by the speeds, distances, and geometry involved.

C. COMPUTATION OF RANGE VARIANCE

The covariance matrix for this type of parameterization has terms for $\dot{X}$, $\dot{Y}$, and A (as well as X and Y) but not for range itself, so the variance of the range, σ_R^2, is not provided directly, but is obtained as follows:

For the bearing-only cases, with R, R_X, and R_Y representing range, and X-and Y-components of range respectively

$$R = (R_X^2 + R_Y^2)^{1/2}$$

so $\frac{\partial R}{\partial R_X} = \frac{R_X}{R}$, and $\frac{\partial R}{\partial R_Y} = \frac{R_Y}{R}$.

The first-order (linear) Taylor Series approximation (where ^ indicates an estimated value) is:

$$R \doteq \hat{R} + \frac{\partial R}{\partial R_X}(R_X - \hat{R}_X) + \frac{\partial R}{\partial R_Y}(R_Y - \hat{R}_Y)$$

therefore

$$\sigma_R^2 \doteq (\frac{\partial R}{\partial R_X})^2\sigma_X^2 + (\frac{\partial R}{\partial R_X})(\frac{\partial R}{\partial R_Y})\mathrm{Cov}(R_X, R_Y) + (\frac{\partial R}{\partial R_Y})^2\sigma_Y^2$$

or, substituting for the partial derivatives,

$$\sigma_R^2 \doteq \frac{1}{R^2}(R_X^2\sigma_X^2 + 2R_XR_Y\mathrm{Cov}(R_X,R_Y) + R_Y^2\sigma_Y^2).$$

Similarly, for the bearing-elevation cases, since

$$R = (R_X^2 + R_Y^2 + R_A^2)^{1/2}$$

then

$$\sigma_R^2 = \frac{1}{R^2}(R_X^2\sigma_X^2 + 2R_XR_Y\mathrm{Cov}(R_X,R_Y) + R_Y^2\sigma_Y^2 + 2R_YR_A\mathrm{Cov}(R_Y,R_A) + R_A^2\sigma_A^2 + 2R_XR_A\mathrm{Cov}(R_X,R_A)).$$

Note that $\mathrm{Cov}(R_X,R_Y) = \mathrm{Cov}(X,Y)$ where X and Y are the target's X and Y coordinate positions, since the fighter (observer) position is known.

APPENDIX B

EKF REFERENCE FRAMES AND MOTION MODELS

A. "FLAT-EARTH" REFERENCE FRAME

The EKF's for both the bearing-only and bearing-elevation observation models are set in a Cartesian coordinate system with axes X, Y and A. This reference system has its origin at 0 altitude directly beneath the fighter at time 0 (time of initial observation), and Y-axis in the direction of the first observed bearing. Bearing and course are measured in the X-Y plane clockwise from the Y-axis.

B. *MOVEMENT IN THE "FLAT-EARTH" MODEL*

Since altitude is held constant for the fighter and the target, movement is a two-dimensional problem. For example if a target is at position (X_1,Y_1,A_1) at time 1, and at time 2 has moved D units on a course of C, then his new position (X_2,Y_2,A_2) is computed by: $X_2 = X_1 + D \sin C$, $Y_2 = Y_1 + D \cos C$, and $A_1 = A_2$.

C. SPHERICAL REFERENCE FRAME

Although the EKF algorithms presented here utilize a Cartesian (flat-Earth) reference frame, the algorithms are also tested using fighter and target positions generated by a spherical model. Here the Earth is modeled as a perfect

sphere of radius 3444 nautical miles. "Constant" course in this model means a great circle track with constant altitude; speed refers to ground speed, i.e., the speed of the object's projection on the Earth's surface.

For computational ease a reference system is again based on fighter location and bearing to the target at time 0. The origin of this (latitude, longitude, altitude) spherical coordinate system is defined as the zero-altitude point directly beneath the fighter at time 0, and the initial observed bearing to the target is defined to be 0. (This may be thought of as shifting the Earth's coordinate system so that the intersection of the equator and the Greenwich Meridian is directly beneath the fighter at time 0, and the first observed bearing is True North).

D. MOVEMENT IN THE SPHERICAL MODEL

In computing movement in the spherical system the following rules of spherical trigonometry are used (refer to Figure B.1):

Law of Sines:

$$\frac{\sin \alpha}{\sin A/E} = \frac{\sin \beta}{\sin B/E} = \frac{\sin \gamma}{\sin C/E}$$

Law of Cosines:

$$\cos B/E = \cos A/E \cos C/E + \sin A/E \sin C/E$$

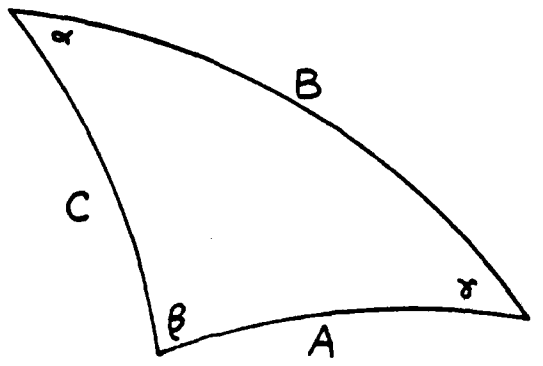

Figure B.1. Spherical Trigonometry Reference

$$\cos \beta = - \cos \alpha \cdot \cos \gamma + \sin \dot{\alpha} \cdot \sin \gamma \cdot \cos B/E$$

where E is the Earth's radius.

If in this coordinate system a target has position (latitude,longitude,altitude) = (X_1,Y_1,A_1) and Great Circle course C_1 at time 1, and if by time 2 it has moved D units at constant altitude, the new position (X_2,Y_2,A_2) and course C_2 are computed by:

$$Y_2 = \sin^{-1}(\sin Y_1 \cdot \cos D + \cos Y_1 \cdot \sin D \cdot \cos C_1)$$

$$X_2 = X_1 + \sin^{-1}(\sin D \cdot \sin C_1 \div \cos Y_2)$$

$$C_2 = (\pi - \cos^{-1}(\sin C_1 \cdot \sin(X_2-X_1) \cdot \sin Y - \cos C_1 \cdot \cos(X_2-X_1)$$

$$\times (C_1 \div |C_1|)$$

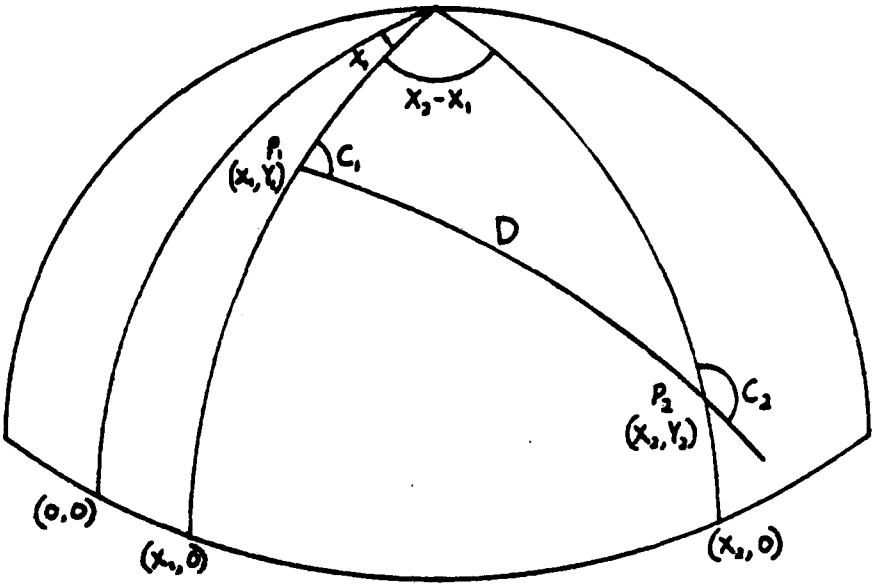

Figure B.2. Spherical Movement

and

$$A_2 = A_1 .$$

APPENDIX C

FIGHTER MANEUVERS

Only one set of fighter maneuvers are analyzed in this study. Some types of maneuvers are certainly better than others and the EKF algorithm has been demonstrated to be robust enough to operate well with a wide variety of different maneuvers; the essential features are that there be some variation in motion parameters [Ref. 9] and that the fighter be able to determine with reasonable precision his own position.

The fighter maneuvers used for these simulations are as follows:

(a) Upon initial target observation he immediately (instantaneously) sets a course 0.7 radians (about 40 degrees) left of the first bearing observation.

(b) The fighter maintains a constant course (constant speed and altitude with no horizontal turns--in the spherical model this is a Great Circle track) until either a pre-set number of new observations have been taken, or until the relative bearing angle to the target exceeds 0.96 radians (about 55 degrees) right. At this time he turns (again instantaneously) to establish a new course 0.7 radians to the right of the most recent bearing observation, and similarly continues until relative bearing exceeds 0.96

radians left or until a set number of observations have been taken.

(c) This not-quite-symmetrical zig-zag pattern continues until a set number of total observations have been recorded or until the target has passed the fighter (bearing observation angle less than $-\frac{\pi}{2}$ or greater than $\frac{\pi}{2}$).

APPENDIX D

ELEVATION ANGLE CORRECTION FOR EARTH'S CURVATURE

The Extended Kalman Filter algorithms proposed here were developed based on a "flat-Earth" motion model. To enhance the performance of the bearing-elevation EKF when using inputs from a spherical motion model, a simple, approximate elevation angle correction was developed.

Referring to the figure on the next page, the notation is as follows:

α = true elevation angle measured from the horizon

α' = "corrected" elevation angle to be input to the EKF

R = line-of-sight range

E = radius of the Earth (assumed here to be 3444nm)

A_T = altitude of target

A_F = altitude of fighter

$\beta = \frac{\pi}{2} + \alpha$.

Then

$$\alpha' \triangleq \left[\frac{A_T - A_F}{R}\right] \text{ by construction}$$

$$\alpha' \doteq \left[\frac{A_T - A_F}{R}\right] \text{ by small angle sine approximation}$$

$$\sin(-\alpha) = \sin\left(\frac{\pi}{2} - \beta\right) = \cos\beta = \left[\frac{R^2 + (E+A_F)^2 - (E+A_T)^2}{2R(E+A_F)}\right]$$

by law of cosines

$$\alpha \doteq \left[\frac{R^2 + (E+A_F)^2 - (E+A_T)^2}{2R(E+A_F)}\right] \text{ by small angle sine approximation}$$

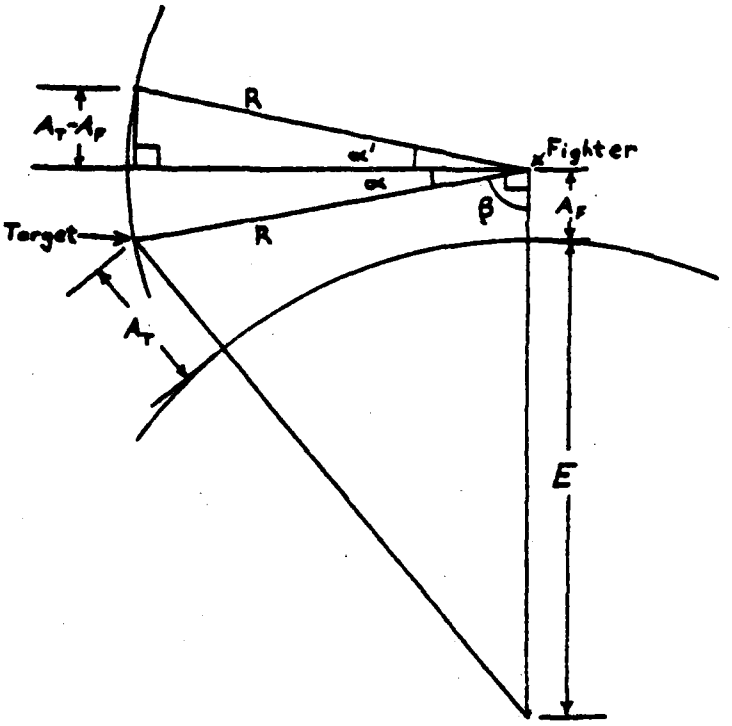

Figure D.1. Elevation Angle Correction

$$\alpha' - \alpha \doteq \left[\frac{A_T - A_F}{R}\right] + \left[\frac{R^2 + (E+A_F)^2 - (E+A_T)^2}{2R(E+A_F)}\right]$$

$$= \frac{R^2 - A_T^2 + 2A_TA_F - A_F^2}{2R(E+A_F)}$$

so, since A_T and A_F are "small" and their difference is "small",

$$\alpha' - \alpha \doteq \frac{R}{2E}$$

so $\alpha' = \alpha + \frac{R}{2E}$ is the correction (based on EKF-estimated range).

NOTE: As the magnitude of $A_T - A_F$ increases relative to range, the approximation becomes less accurate, but as range decreases the correction goes to zero.

APPENDIX E

APL COMPUTER PROGRAM

The APL program shown here assumes global variables as defined in the initial comment section. The program updates fighter and target positions as described in Appendices B and C, generates random observations, and computes corresponding BO and BE EKF estimates. Choice of output variables and programming of output statistics is left to the user.

```
[1]   ⍝ VARIABLE DEFINITIONS
[2]   ⍝   DISTANCES (SPEEDS) ARE IN NM (KTS) ÷3444
[3]   ⍝   ANGLES, COURSES, BEARINGS ARE IN RADIANS
[4]   ⍝   2 AT END OF VARIABLE NAME INDICATES BE (VICE BO)
[5]   ⍝ SIG: INITIAL ESTIMATED   MATRICES (AND AFTER MOVEMENT)
[6]   ⍝ PHI:   MATRICES
[7]   ⍝ SIGM: ESTIMATED   MATRICES AFTER MEASUREMENT
[8]   ⍝ MU: INITIAL ESTIMATED STATE VECTOR (AND AFTER MOVEMENT)
[9]   ⍝ MM: ESTIMATED STATE VECTOR AFTER MEASUREMENT
[10]  ⍝ R1,R2: P DIAGONAL ELEMENTS; Q: Q MATRICES
[11]  ⍝ MM,MV,MR,MX,MA,:
[12]  ⍝ MMU,DM,MM:
[13]  ⍝ RAN: FUNCTION WHICH CALLS A N(0,1) RANDOM NUMBER
[14]  ⍝ DELT: TIME BETWEEN OBSERVATIONS IN HOURS
[15]  ⍝ NN: NUMBER OF OBSERVATIONS BETWEEN TURNS
[16]  ⍝ FX, FY, FA, FS, FCRS: FIGHTER COORDINATES, SPEED, COURSE
[17]  ⍝ LSRG, BRG: TRUE LINE-OF-SIGHT RANGE AND BEARING TO TARGET
[18]  ⍝ TX, TY, TA, TS, TCRS: TARGET COORDINATES, SPEED, COURSE
[19]  ⍝ TXD, TYD: TGT X AND Y VELOCITIES
[20]  ⍝ THRG: TRUE HORIZ RANGE (FLAT-EARTH MOTION MODEL)
[21]  ⍝ GCRG: TRUE GREAT CIRCLE RANGE (SPHERICAL MOTION MODEL)
[22]  ⍝ FRUN, TRUN: DISTANCE COVERED BY FIGHTER, TARGET IN DELT
[23]  ⍝ F = 1 (0) IF ELEVATION CORRECTION APPLIED (NOT APPLIED)
[24]  ⍝ S = 1 (SN = 0) IF USE SPHERICAL MOTION MODEL
[25]  ⍝ S = 0 (SN = 1) IF USE FLAT-EARTH MOTION MODEL
[26]  ⍝ TELA: TRUE ELEVATION ANGLE
[27]  ⍝ VAL = 1 : MU, MU2 INITIALLY RANDOM ABOUT TRUE STATE
[28]  ⍝     = 0 : MU, MU2 SET AT SPECIFIC NUMERIC ESTIMATES
[29]  ⍝
[30]  ⍝ INITIALIZATION
[31]  ⍝
[32]   GCRG←(¯2)⊗(((FA←1)⍟2)+((TA←1)⍟2)-LSRG⍟2)÷2×(FA←1)×TA←1
[33]   THRG←((LSRG⍟2)-(TA-FA)⍟2)⍟0.5
[34]   FRUN←DELT×FS
[35]   TRUN←DELT×TS
[36]   BRG←¯1×MV[1;]←RAN[(2+2×NUM)]×R[1;1]⍟0.5 .
[37]   TCRS←BRG←TCS×(⊗1)÷180
[38]   TX←(S×(¯3)⊗(3⊗GCRG)×1⊗BRG)+SN×THRG×1⊗BRG
[39]   TY←(S×(¯3)⊗|(1⊗TX)×3⊗(⊗0.5)-BRG)+SN×THRG×2⊗BRG
[40]   TXD←TS×1⊗TCRS
[41]   TYD←TS×2⊗TCRS
[42]   TELA←(S×(¯2)⊗(TA←1)×(1⊗GCRG)÷LSRG)+SN×(¯3)⊗(TA-FA)÷THRG
[43]   Z←0,TELA←RAN[(3+2×NUM)]×RR[2;2]⍟0.5
[44]   →L×⍳VAL=0
[45]   RANV←RAN RAN RAN RAN RAN
[46]   MU← 4 1 ⍴MU2← 5 1 ⍴((TS×((1⊗TCRS),2⊗TCRS)),0,THRG,TA)+RANV×SIGRAD⍟0.5
[47]  ⍝
[48]  ⍝ MEASUREMENT
[49]  ⍝
[50]  ⍝ EQUATIONS 2.2 - 2.4 FOR BEARING-ONLY
[51]  L:MR←((((MX←MU[3;])-FX)⍟2)+((MY←MU[4;])-FY)⍟2)⍟0.5
[52]   MMU← 1 1 ⍴(¯3)⊗((MX-FX)÷MY-FY)
[53]   DM← 1 4 ⍴0,0,((MY-FY)÷MR⍟2),(FX-MX)÷MR⍟2
[54]   K←SIG1+.×(⍉DM)+.×⌹((DM+.×SIG1+.×(⍉DM))+R[1;1])
[55]   MM←(4,1)⍴MU+K+.×(((1,1)⍴Z[1])-MV+MMU)
[56]   SIGM←(((4,4)⍴(1,4⍴0))-K+.×DM)+.×SIG1
[57]  ⍝
[58]  ⍝ EQUATIONS 2.2 - 2.4 FOR BEARING-ELEVATION
[59]   MR2←((((MX2←MU2[3;1])-FX)⍟2)+((MY2←MU2[4;1])-FY)⍟2)⍟0.5
[60]   MMU2← 2 1 ⍴((¯3)⊗((MX2-FX)÷MY2-FY)),(¯3)⊗((MA2←MU2[5;])-FA)÷MR2
[61]   DM2←0,0,((MY2-FY)÷MR2⍟2),((FX-MX2)÷MR2⍟2),0,0,0
[62]   DM2←DM2,((FA-MA2)×(MX2-FX)÷(MR2⍟3)÷MR2×(MA2-FA)⍟2)
[63]   DM2←DM2,((FA-MA2)×(MY2-FY)÷(MR2⍟3)÷MR2×(MA2-FA)⍟2)
[64]   DM2← 2 5 ⍴DM2,(MR2)÷((MR2⍟2)÷(MA2-FA)⍟2)
[65]   K2←(SIG2+.×(⍉DM2))+.×⌹((DM2+.×SIG2+.×⍉DM2)+RR)
[66]   MM2← 5 1 ⍴MU2+K2+.×((2 1 ⍴Z)-MV2+MMU2)
[67]   SIGM2←((5 5 ⍴(1,5⍴0))-K2+.×DM2)+.×SIG2
[68]  ⍝ . . .
```

```
[69]  I←I+1
[70]  →LC×I≤NUM
[71]  ⍝
[72]  ⍝ MOVEMENT
[73]  ⍝
[74]  ⍝ EQUATIONS 2.5,2.6 FOR BEARING-ONLY
[75]  LC:HU←(PHI+.×HH)+HH
[76]  SIG1←(PHI+.×SIGH+.×⍉PHI)+⍵
[77]  ⍝
[78]  ⍝ EQUATIONS 2.5,2.6 FOR BEARING-ELEVATION
[79]  HU2←(PHI2+.×HH2)+HH2
[80]  SIG2←(PHI2+.×SIGH2+.×⍉PHI2)+⍵2
[81]  ⍝
[82]  ⍝ UPDATE FLAT EARTH
[83]  ⍝
[84]  →LU×⍳S
[85]  TX←TX+TRUN×1⌽TCRS
[86]  TY←TY+TRUN×2⌽TCRS
[87]  FX←FX+FRUN×1⌽FCRS
[88]  FY←FY+FRUN×2⌽FCRS
[89]  THRS←(((TX-FX)*2)+(TY-FY)*2)*0.5
[90]  LSRS←((THRS*2)+(TA-FA)*2)*0.5
[91]  BRS←(¯3)⌽(TX-FX)+TY-FY
[92]  TELA←(¯3)⌽(TA-FA)+THRS
[93]  →LLU
[94]  ⍝
[95]  ⍝UPDATE SPHERICAL EARTH
[96]  ⍝
[97]  LU:TY←(¯1)⌽((1⌽TY)×2⌽TRUN)+(2⌽TY)×(1⌽TRUN)×TCRS
[98]  FY←(¯1)⌽((1⌽FY)×2⌽FRUN)+(2⌽FY)×(1⌽FRUN)×FCRS
[99]  TX←TX+(¯1)⌽(1⌽TRUN)×1⌽(TXX←TX)+2⌽TYY←TY
[100]  FX←FX+(¯1)⌽(1⌽FRUN)×1⌽(FXX←FX)+2⌽FYY←FY
[101]  TCRS←(×TCRS)×(⍳1)-(¯2)⌽((1⌽TCRS)×(1⌽TX-TXX)×1⌽TYY)-(2⌽TCRS)×2⌽TX-TXX
[102]  FCRS←(×FCRS)×(⍳1)-(¯2)⌽((1⌽FCRS)×(1⌽FX-FXX)×1⌽FYY)-(2⌽FCRS)×2⌽FX-FXX
[103]  SCRS←(¯2)⌽((1⌽TY)×1⌽FY)+(2⌽TY)×(2⌽FY)×2⌽TX-FX
[104]  LSRS←(((FA+1)*2)+((TA+1)*2)-2×(FA+1)×(TA+1)×2⌽SCRS)*0.5
[105]  BRS←(¯1)⌽(2⌽TY)×(1⌽TX-FX)÷1⌽SCRS
[106]  TELA←(¯2)⌽(TA+1)×(1⌽SCRS)+LSRS
[107]  ⍝
[108]  LLU:→JJ×⍳FY<TY
[109]  LP:→0
[110]  JJ:Z←(BRS+RAN[I]×R1),(TELA+RAN[((2×NUM)-I-1)]×R2)+ETRS2×F+2
[111]  J←FCRS
[112]  FCRS←(J×(HH<TURN)∧(|J-Z[1])<0.96)+((Z[1]+0.7)×((HH=TURN)∧((J-Z[1])<0))∨(
J-
       Z[1])≤¯0.96)+(Z[1]-0.7)×((HH=TURN)∧((J-Z[1])>0))∨(J-Z[1])≥0.96
[113]  HH←1+HH×FCRS=J
[114]  →L
       ▼
```

LIST OF REFERENCES

1. Naval Surface Weapons Center, NSWC TR 81-368, Application of a Kalman Filter Passive Targeting Algorithm to Fleet Air Defense, by E.J. Ohlmeyer, November 1982.

2. Stiffler, D.R., Analysis of Six Algorithms for Bearing-Only Ranging in an Air-to-Air Environment, M.S. Thesis, Air Force Institute of Technology, December 1982.

3. Gelb, A., Editor, Applied Optimal Estimation, Analytical Science Corporation, The M.I.T. Press, Cambridge, Mass., 1974.

4. Kalman, R.E., "A New Approach to Linear Filtering and Prediction Problems," J. Basic Eng., v. 82 D, p. 34-45, March 1960.

5. Naval Postgraduate School Report NPS-62Ts77071, Advances in Passive Target Tracking, by H. Titus (editor), May 1977.

6. Daly, P.H., The Kalman Filter and Passive Ranging, M.S. Thesis, Naval Postgraduate School, March 1983.

7. Washburn, A.R., "A Short Introduction to Kalman Filters," (unpublished paper), 1980.

8. Aidala, V.J., "Kalman Filter Behavior in Bearings-Only Tracking Applications," IEEE Transactions on Aerospace and Electronics Systems, v. AES-15, No. 1, pp. 29-39, January 1979.

9. Graham, R.L., The Bearing Regression Approach to Passive Ranging, M.S. Thesis, Naval Postgraduate School, June 1970.

INITIAL DISTRIBUTION LIST

		No. Copies
1.	Defense Technical Information Center Cameron Station Alexandria, Virginia 22314	2
2.	Library, Code 0142 Naval Postgraduate School Monterey, California 93943	2
3.	Professor J.N. Eagle, Code 55Er Naval Postgraduate School Monterey, California 93943	1
4.	Professor N.R. Forrest, Code 55Fo Naval Postgraduate School Monterey, California 93943	1
5.	Professor H. Titus, Code 62Ts Naval Postgraduate School Monterey, California 93943	1
6.	Commanding Officer Attn: Dr. C.E. Dickerson CNA(OEG) Air Test and Evaluation Squadron Four Naval Air Station Pt. Mugu, California 93042	1
7.	Mr. E.J. Ohlmeyer, Code G23 Naval Surface Weapons Center Dahlgren, Virginia 22448	1
8.	Commander Naval Air Development Center Attn: Harvey Sokoloff, Code 3011 Warminster, Pennsylvania 18974	1
9.	Cdr. Ward H. Ewing, Code 07P5 Office of Naval Technology Rm 811 800 North Quincy Street Arlington, Virginia 22217	2
10.	Mrs. Dorothy Ewing, Code MOM 204 Pine Street Glendive, Montana 59330	1